Optics Letters

Progress toward an efficient, uniformly scalable lithium niobate terahertz pulse source

Gergő Krizsán,[1,2,3,*] Bálint Jurasits,[1] Gábor Almási,[1] and János Hebling[1,2]

[1] Institute of Physics, University of Pécs, Ifjúság ú. 6, Pécs 7624, Hungary
[2] Szentágothai Research Centre, University of Pécs, Ifjúság ú. 6, Pécs 7624, Hungary
[3] HUN-REN–PTE High-Field Terahertz Research Group, Pécs, Hungary
*krizsan@fizika.ttk.pte.hu

Received 23 March 2025; revised 2 June 2025; accepted 3 June 2025; posted 4 June 2025; published 20 June 2025

We report significant progress in developing a compact, imaging-free, and scalable tilted-pulse-front-pumped (TPFP) terahertz (THz) source based on a nonlinear echelon slab. The slab thickness- and pump intensity-dependent THz generation efficiency have been characterized, reaching an efficiency of ~0.085%, which is ~2.8× higher than previously. The impact of microstructure quality shows that surface roughness reduces efficiency by lowering diffraction efficiency and increasing beam divergence. A simple theoretical model is introduced, which shows good agreement with experimental results and predicts significantly higher efficiency—exceeding 0.65% (2%) at room (cryogenic) temperature—with refined microstructure quality.

© 2025 Optica Publishing Group under the terms of the Optica Open Access Publishing Agreement

https://doi.org/10.1364/OL.563154

Terahertz (THz) pulse applications, such as strong-field control of matter [1] and charged particle manipulation and acceleration [2–5], require high field strengths. Achieving this requires high pulse energy and excellent focusability. Conventional tilted-pulse-front-pumped (TPFP) setups using lithium niobate (LN) prisms have produced the highest THz pulse energies and field strengths in the low-frequency range (<2 THz). However, the scalability of such setups is limited by (i) imaging errors and pulse duration broadening at the edges of a large pump beam [6] and (ii) the prism-shaped LN crystal with a large (63°) wedge angle [7]. In recent years, several novel setups have been proposed to mitigate or eliminate these limitations [8–14]. One such setup employs only a plan-parallel nonlinear echelon slab (NLES) in combination with a volume phase holographic grating (VPHG) [14], eliminating both (i) and (ii).

The first experimental demonstration of the NLES-VPHG setup used a small-scale NLES, and the device was not fully characterized.

In this Letter, we present a comprehensive characterization of an NLES-VPHG setup incorporating a larger NLES. More importantly, we investigate the dependence of THz generation efficiency on the NLES thickness and compare the results with theoretical model calculations.

The setup was described in detail in Ref. [13], and its schematic drawing is shown in Fig. 1. The VPHG introduces the required pulse-front tilt (PFT), and the LN NLES generates THz pulses by optical rectification.

The pump beam reaches the VPHG at normal incidence and is efficiently diffracted into a single order. The diffraction angle and the PFT angle γ are equal and are given by the grating equation, which in this case simplifies to $\sin\gamma = \lambda/d$, where λ is the pump wavelength in vacuum and d is the grating period. The pump beam then enters the NLES at normal incidence to the input facets of the echelon steps. Upon entry, the pulse front becomes segmented. While the average PFT angle remains unchanged, the γ_{LN} tilt angle of each segment is determined by the following equation: $\tan(\gamma_{LN}) = \tan(\gamma)/n_{g,LN}$, where $n_{g,LN}$ is the group refractive index of LN. The generated THz radiation propagates perpendicular to the average pulse front and exits the NLES perpendicularly to its backside.

The same laser source and VPHG were used as in the previous experiment. The pump pulses had a 1030 nm central wavelength, a 200 fs transform-limited pulse duration, and energy up to 1 mJ. The VPHG had a line density of 860 lines/mm and lacked AR coatings on both sides, resulting in ~22% Fresnel loss. The measured external diffraction efficiency was ~76%.

Since the duration of a Fourier-limited pulse rapidly increases behind the VPHG, pre-chirping was necessary to maintain the shortest pulse duration—and thus the highest intensity—inside the NLES. This was achieved by adjusting the distance between the pulse compression gratings of the pump laser. The highest THz energy was obtained when the pulse duration in front of the VPHG was 1 ps (with slight variations depending on the NLES thickness).

For the experiment, two new NLES samples were fabricated from congruent LN with 5% Mg doping. Both had identical dimensions: 20 mm height (parallel to the echelon grooves), 30 mm width, and $L = 6$ mm thickness. Similar to the earlier experiment [13], the echelon step structure on the entrance surface of the NLES was fabricated by micromachining with a diamond tool, producing step sizes of $w = 50$ μm and $h = 98$ μm.

THz energy was measured using a calibrated pyroelectric detector (Sensor und Lasertechnik, THz 30). To eliminate the fundamental and second-harmonic beams, a PTFE (Teflon) window and two black paper filters were placed between the NLES

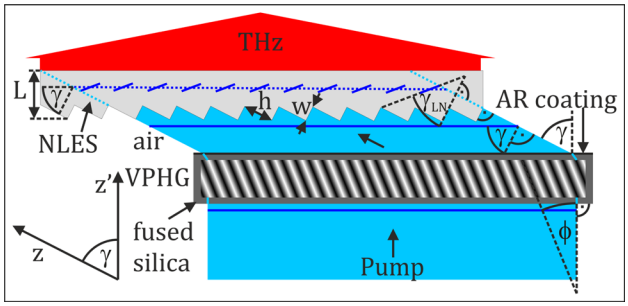

Fig. 1. Schematic drawing of the NLES-VPHG setup.

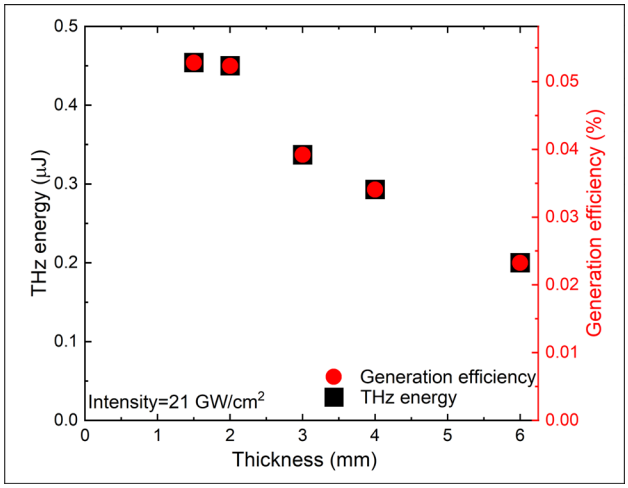

Fig. 2. Generated THz energy and THz generation efficiency versus the NLES thickness.

and the detector. The THz transmission of these filters was carefully measured and accounted for in the energy calculations.

In these experiments, the setup was optimized for maximum THz energy. Initially, both 6 mm thick NLES samples exhibited the same generation efficiency within the error margin. After verifying this (including when different parts of the microstructure were illuminated), one NLES (No. 1) was polished to 4 mm, while the other (No. 2) was thinned to 3 mm. After measuring the THz energy and generation efficiency, No. 1 was further polished to 2 mm and No. 2 to 1.5 mm.

Figure 2 presents the dependence of generation efficiency on the NLES thickness. During these measurements, the pump beam size was 7.5×6.5 mm ($1/e^2$). The indicated 21 GW/cm^2 peak intensity refers to the value before the VPHG, assuming a Fourier-limited pulse duration.

As seen in Fig. 2, within the investigated NLES thickness range, the generation efficiency and THz energy increase as the thickness decreases. At room temperature, the NLES crystal with a 1.5 mm thickness exhibited the highest generation efficiency.

Figure 3 shows the THz energy and generation efficiency for different pump energies and intensities in the case of the 2 mm thick NLES. In this measurement, the pump beam size was reduced to $\sim 7.5 \times 1.5$ mm ($1/e^2$) to achieve higher maximum pump intensity. The obtained THz generation efficiency increased monotonically over the entire intensity range, but above ~50 GW/cm^2, the intensity dependence became modest. The maximum efficiency of ~0.085% was reached at the highest available intensity of ~103 GW/cm^2.

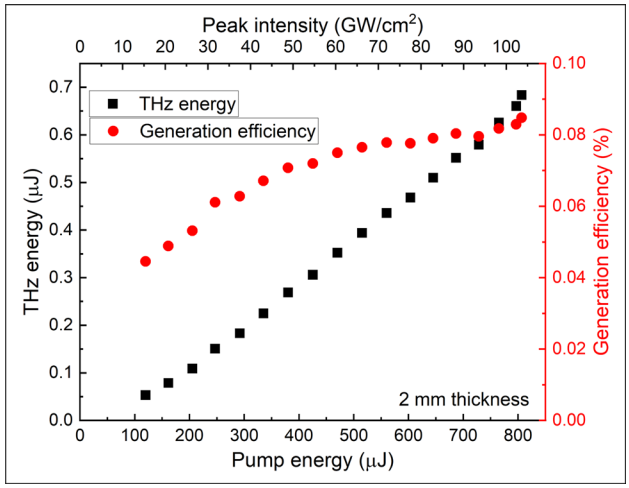

Fig. 3. Generated THz energy and THz generation efficiency for the 2 mm thick NLES as a function of pump energy (bottom scale) and intensity (top scale).

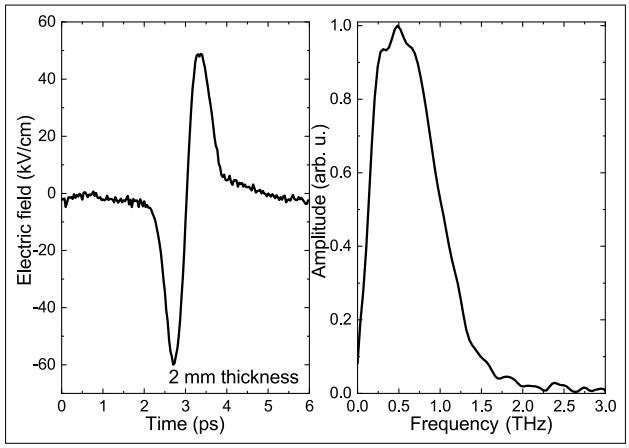

Fig. 4. (a) THz waveform measured by electro-optic sampling. (b) Corresponding calculated amplitude spectrum.

For electro-optic measurement, a 0.1 mm thick (110)-oriented (active) GaP crystal was used, sandwiched with a 1 mm thick (001)-oriented (inactive) GaP crystal. The pump beam size was reverted to $\sim 7.5 \times 6.5$ mm ($1/e^2$). The measured E-field shape of the THz pulse and the calculated amplitude spectrum are shown in Fig. 4. The generated THz pulse exhibited an almost perfectly single-cycle waveform, with a pulse duration of ~1.2 ps (FWHM). The spectral peak of the measured THz pulses was at ~0.5 THz, with a spectral amplitude FWHM of ~0.9 THz. It is worth noting that the ~1 ps probe pulse duration lowers the measured frequency. According to our calculations, the actual spectral peak was at ~0.6 THz.

The THz beam size was measured immediately after the NLES using the knife-edge technique and was found to be $\sim 5.8 \times 4.5$ mm. Based on this beam size, the measured THz energy, and the measured waveform, the peak electric field strength of the radiation immediately after the NLES was calculated to be ~59 kV/cm.

Since the efficiency of the NLES-VPHG setup strongly depends on the quality of the micro-machined entrance surface of the NLES, we investigated it using two methods. According to

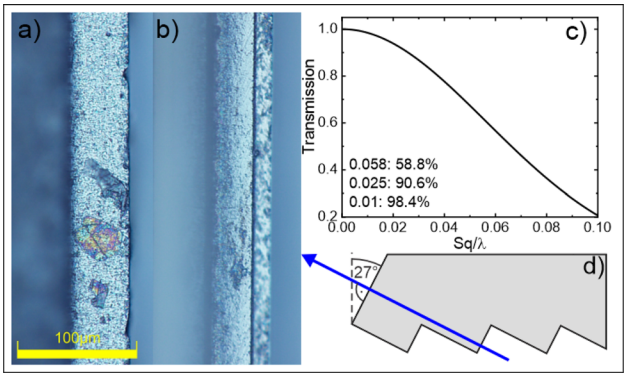

Fig. 5. Images of NLES steps: (a) from the new NLES with larger surface and (b) from the older prototype NLES with smaller surface. (c) Transmission dependence on Sq normalized by the wavelength. (d) Schematic illustration of the polished edge of the NLES for microstructure quality measurements.

optical microscope measurements (Olympus DSX510), the root mean square roughness S_q measured over a 30×30 µm area was ~53 nm. A very similar value was measured for the previously used prototype NLES, but in that case, a visible line appeared in every step. A picture of one of the steps of both NLES is shown in Figs. 5(a) and 5(b).

To obtain further independent information on the microstructure quality, diffraction efficiency measurements were performed. For this purpose, one side surface of the NLES was polished at 27°, as indicated in Fig. 5(d). It was then directly illuminated near this end at normal incidence to the input facets of the echelon steps. The main diffraction order of the pump also exited the NLES perpendicularly.

In the case of perfect microstructure quality, considering the Fresnel losses on both the input and output surfaces of the NLES, the expected transmission through the NLES is ~75.1%. Using a 200 fs pumping pulse (CW laser light), the main diffraction order should contain ~90% (~80%) of the transmitted power, or ~68% (~61%) of the input power. (The difference between the expected diffraction efficiencies for the two types of lasers is described in detail in Ref. [14].) However, the measured power in the main order was lower than these values. For both NLES, the mainlobe contained ~40% (~38%) of the input pulsed (CW) laser power. Diffraction efficiency measurements were performed at several positions (top, middle, and bottom of the NLES). The measured diffraction efficiencies were nearly identical at these positions, indicating that the microstructure quality remains constant along the vertical direction. Additionally, based on visual inspection of the scattered light, the surface quality appears constant along the horizontal direction as well. Based on these results, with a microstructure having a smoother surface, an energy increase of 68%/40% = 1.7× (61%/38% = 1.6×) could be achieved in the main diffraction order.

According to Eq. (1) of Ref. [15], the dependence of transmission through a rough surface, normalized by the transmission through a perfectly smooth surface, is given by

$$T = \exp\left(-\frac{4\pi S_q}{\lambda}\right)^2, \tag{1}$$

Equation (1) is plotted in Fig. 5(c). As shown, the predicted normalized transmission is equal to the measured 40%/68% = 0.59 (38%/61% = 0.62) value for a normalized roughness of $S_q/\lambda \approx 0.058\,(0.055)$. Thus, based on the transmission measurement, the roughness is calculated as $S_q = S_q/\lambda \cdot \lambda = 0.058\,(0.055) \times 1030\,\text{nm} \approx 60\,(57)$ nm. These values are in good agreement with the previously mentioned 53 nm roughness measured by optical microscopy. According to Eq. (1), decreasing the surface roughness from ~60 nm to 25 nm (10 nm) could result in a ~55% (~67%) increase in transmission. Due to the nonlinearity of the THz generation process, an even larger increase is expected in the THz generation efficiency.

In addition to reducing the energy contained in the main diffraction order, imperfect microstructuring can also increase its divergence, further impacting generation efficiency. Beam size measurements indicate that the beam had a horizontal divergence angle larger than expected for a 50 µm slit. The measured horizontal divergence was ~43 mrad, corresponding to a ~30 µm slit size. Since the beam size expands more rapidly after the microstructure, the intensity—and consequently, the THz generation efficiency—decreases.

A simple model was created to compare the measured η_{THz} THz generation efficiency with the theoretical predictions, resulting in the following formula for efficiency [16]:

$$\eta_{\text{THz}} = \frac{2\Omega^2 d_{\text{eff}}^2 I t_{\text{THz}}}{\varepsilon n_{\text{NIR}}^2 n_{\text{THz}} c^3} \exp\left(-\frac{\alpha_{\text{THz}} L}{2}\right) \frac{\sinh^2\left(\frac{\alpha_{\text{THz}} L}{4}\right)}{\left(\frac{\alpha_{\text{THz}} L}{4}\right)^2} \times \left(\int_0^L f(z')g(z')dz'\right)^2, \tag{2}$$

where Ω is the central THz angular frequency, d_{eff} is the effective nonlinear coefficient of LN, I is the average intensity inside the NLES, t_{THz} is the transmission of the THz at the LN–air boundary, ε is the vacuum permittivity, n_{NIR} and n_{THz} are the refractive indices at the optical and THz frequencies, c is the speed of light, α_{THz} is the THz absorption coefficient at the central frequency, and L is the thickness of the NLES. The functions $f(z')$ and $g(z')$ describe effects related to the beam segments [7].

The function $f(z') = \frac{w}{w'(z')}$, where $w'(z')$ is the size of a segment perpendicular to the z axis at the propagation distance z' in the NLES, describes the decrease in intensity due to the increasing segment size with propagation. The function $g(z') = \text{sinc}(\pi x)$, where $x = w'(z')\sin(\gamma)(1 - 1/n_g)n_{\text{THz}}/\lambda_{\text{THz}}$ describes the relative decrease of the generated THz field with respect to a non-segmented pump pulse front [10].

For the efficiency calculations, the step size w was assumed to be 50 µm, but the beam segments expanded according to the measured horizontal divergence of the transmitted pump beam. The average intensity was calculated as follows: $I = I_{\text{peak}}\eta_{\text{VPHG}}t_{\text{NIR}}\eta_{\text{M}}/2$, where η_{VPHG} is the diffraction efficiency of the VPHG, t_{NIR} is the transmission of the optical beam at the air–NLES boundary, and η_{M} is the microstructure diffraction efficiency.

In Fig. 6, the calculated THz generation efficiency is plotted as a function of the NLES thickness, together with the measured efficiencies. As can be seen, the simple model accurately predicts the measured shape of the THz efficiency dependence on the NLES thickness, including the position of its maximum. According to the theory, a slightly thicker NLES (2.15 mm) would yield the highest generation efficiency, compared to the experimentally obtained 1.5–2 mm range. The predicted value of the efficiency maximum is approximately twice as large as the

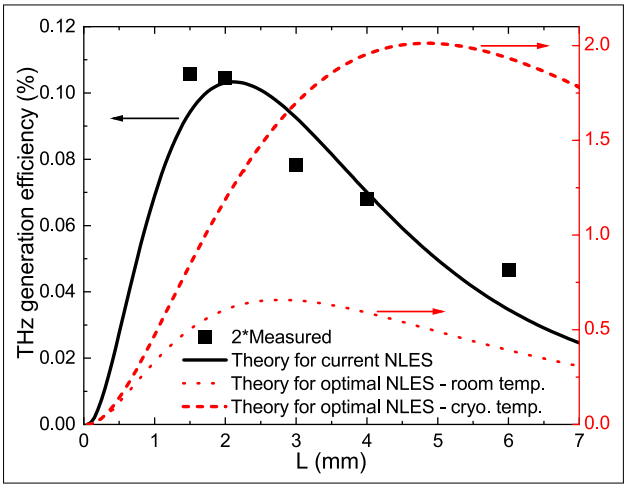

Fig. 6. THz generation efficiency calculations for the current and optimal surface conditions, along with the measured results.

measured one. However, due to the small pump spot size, spatial walk-off—neglected in the model—accounts for a reduction by a factor of about 1.5 [17]. Among the other effects neglected in the theoretical model [18], group-velocity dispersion and, most importantly, the temporal wings of the pump pulse caused by scattering likely account for the remaining ∼35% difference between the theoretical and experimental efficiencies. These two effects may also explain the small but noticeable difference between the predicted and measured positions of the efficiency maximum.

Because of the accurate predictive capability of the theory, it is valuable for making reliable predictions. With AR coatings on both sides of the VPHG, an AR layer on the backside of the NLES for THz, and perfect microstructure quality, the model predicts a THz generation efficiency of ∼0.65% at room temperature and ∼2% at 100 K (see the corresponding curves in Fig. 6). It is worth noting that micromachining LN with an average roughness of ∼10 nm [19] or even ∼1 nm [20] has already been demonstrated.

Furthermore, it is also noteworthy that pumping the presented (optimal) setup at room temperature with a pump beam having a 20 mm × 30 mm elliptical cross section (matching to the size of the used NLES) and pulses with 64 mJ energy and 200 fs duration (corresponding to an intensity of 150 GW/cm^2, significantly below the damage threshold of the NLES), the THz generation efficiency would exceed 0.12% (0.65%) (approaching (significantly exceeding) the 0.16% measured for a conventional TPFP LN source using the same pump laser and THz detector), yielding a THz energy of 77 (416) μJ. Focusing this THz beam by a NA = 0.6 numerical aperture optic would result in an electric field as high as ∼1.7 MV/cm (∼4.5 MV/cm).

In conclusion, using the NLES-VPHG setup—a compact, imaging-free, and scalable THz source—single-cycle THz pulses with an energy of 0.7 μJ and a central frequency of 0.6 THz were generated using 0.86 mJ, 200 fs pump pulses, achieving an efficiency of ∼0.085%. This efficiency is ∼2.8× higher than that achieved in the first demonstration [13]. The primary factors contributing to the efficiency increase are the increased pump intensity and the optimized (thinner) NLES thickness. By utilizing the full (20 mm × 30 mm) area of the NLES with a 60 mJ pump energy, the efficiency is expected to increase to 0.12%, with a corresponding THz energy above 70 μJ. The measured dependence of THz generation efficiency on the NLES thickness aligns well with numerical predictions that incorporate the measured 50 nm roughness of the microstructured NLES surface. The theory predicts efficiencies as high as 0.65% at room temperature and 2.0% at 100 K for <10 nm surface roughness. Due to their excellent focusability, single-cycle waveform, and uniform beam cross section, the THz pulses generated by this scalable setup meet the requirements for applications such as particle acceleration.

Funding. National Research, Development and Innovation Office (2018-1.2.1-NKP-2018-00010, TKP2021-EGA17); HORIZON EUROPE European Innovation Council (101046504).

Acknowledgment. Gergő Krizsán acknowledges support from the EKÖP-24-4 University Research Grant Programme, funded by the Ministry of Culture and Innovation and the National Research, Development and Innovation Fund.

Disclosures. The authors declare no conflicts of interest.

Data availability. The data that support the findings of this study are available within the Letter and from the corresponding author upon reasonable request.

REFERENCES

1. P. Salén, M. Basini, S. Bonetti, *et al.*, Phys. Rep. **836**, 1 (2019).
2. E. Curry, S. Fabbri, J. Maxson, *et al.*, Phys. Rev. Lett. **120**, 094801 (2018).
3. M. T. Hibberd, A. L. Healy, D. S. Lake, *et al.*, Nat. Photonics **14**, 755 (2020).
4. Z. Tibai, S. Turnár, G. Tóth, *et al.*, Opt. Express **30**, 32861 (2022).
5. D. Zhang, Y. Zeng, M. Fakhari, *et al.*, Appl. Phys. Rev. **9**, 031407 (2022).
6. L. Tokodi, J. Hebling, and L. Pálfalvi, J. Infrared, Millimeter, Terahertz Waves **38**, 22 (2017).
7. G. Tóth, L. Pálfalvi, J. A. Fülöp, *et al.*, Opt. Express **27**, 7762 (2019).
8. B. K. Ofori-Okai, P. Sivarajah, W. Ronny Huang, *et al.*, Opt. Express **24**, 5057 (2016).
9. L. Pálfalvi, Z. Ollmann, L. Tokodi, *et al.*, Opt. Express **24**, 8156 (2016).
10. L. Pálfalvi, G. Tóth, L. Tokodi, *et al.*, Opt. Express **25**, 29560 (2017).
11. G. Tóth, L. Pálfalvi, Z. Tibai, *et al.*, Opt. Express **27**, 30681 (2019).
12. L. Guiramand, J. Nkeck, X. Ropagnol, *et al.*, Photonics Res. **10**, 340 (2022).
13. G. Krizsán, Z. Tibai, G. Tóth, *et al.*, Opt. Express **30**, 4434 (2022).
14. G. Krizsán, G. Polónyi, T. Kroh, *et al.*, Opt. Lett. **48**, 3777 (2023).
15. H. E. Bennett and J. Porteus, J. Opt. Soc. Am. **51**, 123 (1961).
16. J. Hebling, K.-L. Yeh, M. C. Hoffmann, *et al.*, J. Opt. Soc. Am. B **25**, B6 (2008).
17. P. S. Nugraha, G. Krizsán, C. Lombosi, *et al.*, Opt. Lett. **44**, 1023 (2019).
18. K. Ravi, W. R. Huang, S. Carbajo, *et al.*, Opt. Express **22**, 20239 (2014).
19. D. Huo, Z. J. Choong, Y. Shi, *et al.*, J. Micromech Microeng. **26**, 095005 (2016).
20. R. Takigawa, E. Higurashi, T. Kawanishi, *et al.*, Opt. Express **22**, 27733 (2014).